

# MIDA boronates are hydrolysed fast and slow by two different mechanisms

Jorge A. Gonzalez<sup>1</sup>, O. Maduka Ogba<sup>2</sup>, Gregory F. Morehouse<sup>3</sup>, Nicholas Rosson<sup>2</sup>, Kendall N. Houk<sup>4</sup>, Andrew G. Leach<sup>5</sup>, Paul H.-Y. Cheong<sup>2\*</sup>, Martin D. Burke<sup>3\*</sup> and Guy C. Lloyd-Jones<sup>1\*</sup>

**MIDA boronates (*N*-methylimidodiacetic boronic acid esters) serve as an increasingly general platform for small-molecule construction based on building blocks, largely because of the dramatic and general rate differences with which they are hydrolysed under various basic conditions. Yet the mechanistic underpinnings of these rate differences have remained unclear, which has hindered efforts to address the current limitations of this chemistry. Here we show that there are two distinct mechanisms for this hydrolysis: one is base mediated and the other neutral. The former can proceed more than three orders of magnitude faster than the latter, and involves a rate-limiting attack by a hydroxide at a MIDA carbonyl carbon. The alternative ‘neutral’ hydrolysis does not require an exogenous acid or base and involves rate-limiting B–N bond cleavage by a small water cluster,  $(H_2O)_n$ . The two mechanisms can operate in parallel, and their relative rates are readily quantified by  $^{18}O$  incorporation. Whether hydrolysis is ‘fast’ or ‘slow’ is dictated by the pH, the water activity and the mass-transfer rates between phases. These findings stand to enable, in a rational way, an even more effective and widespread utilization of MIDA boronates in synthesis.**

**N**-methylimidodiacetic acid esters (1) of boronic acids (2) ('MIDA boronates') have emerged as an increasingly general and automated platform for small-molecule synthesis based on building blocks<sup>1</sup> (Fig. 1a). One of the most important and yet poorly understood features that enables such utility is the distinct rates of hydrolysis for MIDA boronates under various basic conditions<sup>2,3</sup>. When ethereal solutions of MIDA boronates are treated with aqueous NaOH, they are hydrolysed within minutes at room temperature<sup>2</sup>, whereas with aqueous  $K_3PO_4$ , slow hydrolysis takes several hours at elevated temperatures<sup>3</sup> (Fig. 1b). When performing cross-couplings of boronic acids (2) in the presence of anhydrous  $K_3PO_4$ , MIDA boronates (1) undergo little or no hydrolysis, even though small amounts of water are presumably formed via boronic acid oligomerization<sup>2</sup>.

In contrast to other boronates<sup>4</sup>, MIDA hydrolysis rates are remarkably insensitive to the structure of the organic fragment<sup>2,3</sup>, and this generality has enabled these dramatic rate differences to be harnessed to great effect. The lack of hydrolysis under conditions that promote cross-coupling combined with a fast hydrolysis by NaOH collectively enable iterative syntheses of small molecules from a wide range of halo-MIDA boronate building blocks in a manner analogous to iterative peptide coupling<sup>2,5</sup>. Harnessing this approach, many different types of natural products (including highly complex macrocyclic and polycyclic structures), biological probes, pharmaceuticals and materials components have now been prepared using just one reaction iteratively<sup>1</sup>. A machine has also been created that can execute such building-block-based small-molecule construction in a fully automated fashion<sup>6</sup>. With suitably active catalysts, the slow hydrolysis of MIDA boronates can release boronic acids at a rate that avoids their accumulation during cross-coupling. Using this approach, substantial improvements in yields have been achieved with MIDA boronates as

stable surrogates for unstable boronic acids<sup>3</sup>, including the notoriously unstable but very important 2-pyridyl systems<sup>7</sup>. Careful modulation of the extent of the base hydration can also be used to control the hydrolysis and thus speciation in mixtures of boron reagents, which allows selective cross-coupling followed by MIDA redistribution<sup>8</sup>. Collectively, these findings have provided substantial momentum towards a general and automated approach for small-molecule synthesis.

Understanding the mechanism(s) by which these distinct rates of hydrolysis occur is critical, however, to address three areas of current limitations of this platform (Fig. 1a) and thereby maximize its generality and impact. First, MIDA boronates can undergo undesired hydrolysis during selective cross-couplings. For example, iterative cross-couplings with the more-challenging  $Csp^2$  centres that are performed at higher temperatures and/or longer reaction times can be accompanied by undesired MIDA hydrolysis and thus sub-optimal yields are obtained. Generalized iterative couplings with  $sp^3$ -hybridized carbon and heteroatoms would be highly enabling<sup>9,10</sup>, but such reactions can require even more forcing conditions, which cause extensive MIDA hydrolysis. Transitioning this iterative cross-coupling platform to a flow-chemistry format would open up many additional opportunities, and boronates that are stable under aqueous basic cross-coupling conditions would substantially facilitate this transition. Second, MIDA boronates can undergo undesired hydrolysis during building-block synthesis. For example, executing iterative cross-coupling-based syntheses requires access to complex boron-containing building blocks, and doing so from simpler MIDA boronate starting materials plays an important role in this process<sup>11</sup>. However, such transformations can be hindered by competitive hydrolysis during various reactions, workups and/or purifications. MIDA boronate hydrolysis under various mixed-phase HPLC conditions can also hinder analysis. Third,

<sup>1</sup>EaStCHEM, School of Chemistry, University of Edinburgh, Edinburgh, EH9 3FJ, UK. <sup>2</sup>Department of Chemistry, Oregon State University, Corvallis, Oregon 97331, USA. <sup>3</sup>Department of Chemistry, University of Illinois, 454 RAL, Box 52-5 600 South Mathews Avenue, Urbana, Illinois 61801, USA. <sup>4</sup>Department of Chemistry and Biochemistry, University of California, Los Angeles, 607 Charles E. Young Drive East, Los Angeles, California 90095-1569, USA. <sup>5</sup>School of Pharmacy and Biomolecular Sciences, Liverpool John Moores University, Byrom Street, Liverpool L3 3AF, UK.

\*e-mail: paulc@science.oregonstate.edu; mdburke@illinois.edu; guy.lloyd-jones@ed.ac.uk

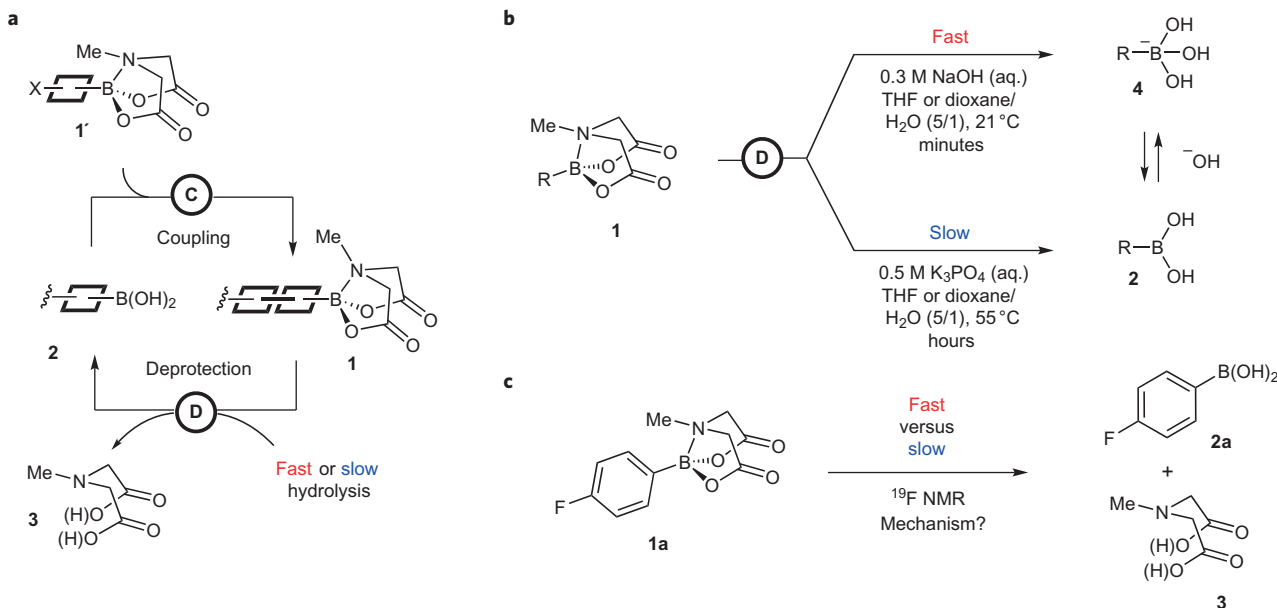


**Figure 1 | Hydrolytic deprotection and coupling of MIDA boronates.** **a**, Iterative coupling platform for small-molecule synthesis from MIDA boronate (**1**) building blocks. Current limitations include suboptimal generality and/or the fine-tuning of hydrolysis rates during deprotections, and undesired hydrolysis during building-block syntheses and selective cross-coupling; these all stand to benefit from a better understanding of the mechanism(s) of MIDA boronate hydrolysis. **b**, Deprotection of MIDA boronates (**1**) under fast and slow conditions,  $k_{\text{rel}} \geq 3 \times 10^3$  at 21 °C in homogeneous THF/H<sub>2</sub>O. **c**, Fluorinated substrate (**1a**) selected for mechanistic investigation, including kinetics, pH profile, homo/heterogeneity, Hammett  $\rho$ ,  $\Delta S^\ddagger$ , site of cleavage (<sup>18</sup>O), water activity, <sup>2</sup>H, <sup>11</sup>B, <sup>13</sup>C and <sup>15</sup>N KIEs, and DFT (M06-2X/6-31G\* and M06L/6-311++G\*\*).

MIDA boronates sometimes demonstrate suboptimal generality and/or capacity for fine-tuning of their hydrolysis rates during deprotections. For example, when deprotections are performed using aqueous ethereal NaOH some MIDA boronates initially hydrolyse rapidly and then relatively slowly, and so require extended reaction times for a complete hydrolysis. Eliminating such effects would substantially enable efforts towards faster and more generalized automation. There are also cases in which finely tuned increases or decreases in boronate hydrolysis rates would enable the slow-release cross-coupling strategy to be more effective and/or boron-selective deprotections of polyboronated intermediates to be achieved. For all of these reasons, we set out to understand the mechanism(s) by which MIDA boronates hydrolyse, both fast and slow.

## Results

**Distinction of limiting mechanisms for ‘fast’ and ‘slow’ release.** After preliminary tests with alkyl and aryl MIDA boronates, we focussed on **1a** (Fig. 1c) using *in situ* <sup>19</sup>F NMR to analyse a range of conditions (A to G (Fig. 2a)). We began with the study of fast release<sup>2</sup> (conditions A), in which a key aspect is the heterogeneity of the medium: the addition of aqueous NaOH to a vigorously agitated solution of **1a** in tetrahydrofuran (THF) generates a metastable emulsion. If the addition rates are too fast, phase separation begins to occur. A full phase separation leads to precipitous reductions in the hydrolysis rates ( $\sim 10^{-3}$ , conditions B and C).

The slow-release conditions<sup>3</sup> (aqueous K<sub>3</sub>PO<sub>4</sub>, 7.5 equiv.) rapidly induce a full phase separation, with less than 3% hydrolysis of **1a** occurring prior to this, irrespective of the stirring rate (conditions D and E). Hydrolysis of **1a** proceeds in the absence of any exogenous base (conditions F) and does so faster than under slow-release conditions (D). This phenomenon arises from partial dehydration of the organic phase by the K<sub>3</sub>PO<sub>4</sub> (Fig. 2c).

We also tested strongly acidic conditions (pH = 0, conditions G). These induce only modest rate accelerations (about fivefold (see Supplementary Fig. 26)). Three distinct hydrolytic regimes (Fig. 1b) were thus identified: acidic ( $k_{\text{H}^+}$ ), neutral ( $k_0$ ) and basic ( $k_{\text{OH}}$ ).

Further insight came from <sup>13</sup>C{<sup>1</sup>H} NMR analysis of the MIDA ligand liberated by hydrolysis of [<sup>13</sup>C<sub>2</sub>]-**1a** in THF/H<sub>2</sub><sup>18</sup>O (9.1 M) (Fig. 2d). Two distinct reactivity patterns emerged: under basic or acidic homogeneous conditions (A and G), hydrolysis leads to mono <sup>18</sup>O incorporation, whereas under neutral conditions (F) there is no significant <sup>18</sup>O incorporation. For conditions B to E, intermediate between strongly basic and neutral, a quantifiable transition between the two outcomes is evident. Importantly, it can be seen that the slow release with K<sub>3</sub>PO<sub>4</sub> (conditions D and E) predominantly, but not exclusively, proceeds via neutral hydrolysis, with the mixing efficiency dictating the base transport rates into the upper organic phase, and in turn, the extent of <sup>18</sup>O incorporation (6–25%).

In the context of MIDA boronate hydrolysis for cross-coupling<sup>2,3</sup>, there are thus two competing processes to consider: neutral ( $k_0$ ) and basic ( $k_{\text{OH}}$ ). Base-mediated hydrolysis is by far the fastest ( $> 10^3$ -fold), provided that an emulsive state is attained by vigorous agitation during the dispersive slow addition of the NaOH. These conditions result in C–O cleavage in just one of the two esters in **1a**, as identified by single <sup>18</sup>O incorporation in **3**. Neutral hydrolysis solely cleaves [B–OC(O)] bonds, which results in no <sup>18</sup>O incorporation in **3** at all.

**Rate laws for basic ( $k_{\text{OH}}$ ) and neutral ( $k_0$ ) hydrolysis.** The kinetics of fast release ( $k_{\text{OH}}$ ) were determined by ultraviolet-visible absorption spectrophotometry at low reactant concentrations using stopped-flow techniques (Fig. 3a). The data are indicative of a rate-limiting attack by a single hydroxide (rate =  $k_{\text{OH}}[\mathbf{1a}][\text{NaOH}]$ ,  $k_{\text{OH}} = 6.1 \text{ M}^{-1} \text{ s}^{-1}$ ), with **1a** being similarly reactive to a *p*-NO<sub>2</sub>-benzoate ester<sup>12</sup>. A linear free-energy relationship for  $k_{\text{OH}}$  was established across a series of Ar-B(MIDA) substrates. In the context of attack by hydroxide, the relative insensitivity of the aromatic ring ( $\log(k_X/k_H) = 0.5\sigma$ ;  $k_X$  is the rate of substituted arene and  $k_H$  is the rate of phenyl substrate) weighs strongly against a pathway that involves the rate-limiting generation of a boronate anion. The acid-catalysed pathway (G in Fig. 2) is even less sensitive to aryl substitution,  $\log(k_X/k_H) \leq 0.01\sigma$ .

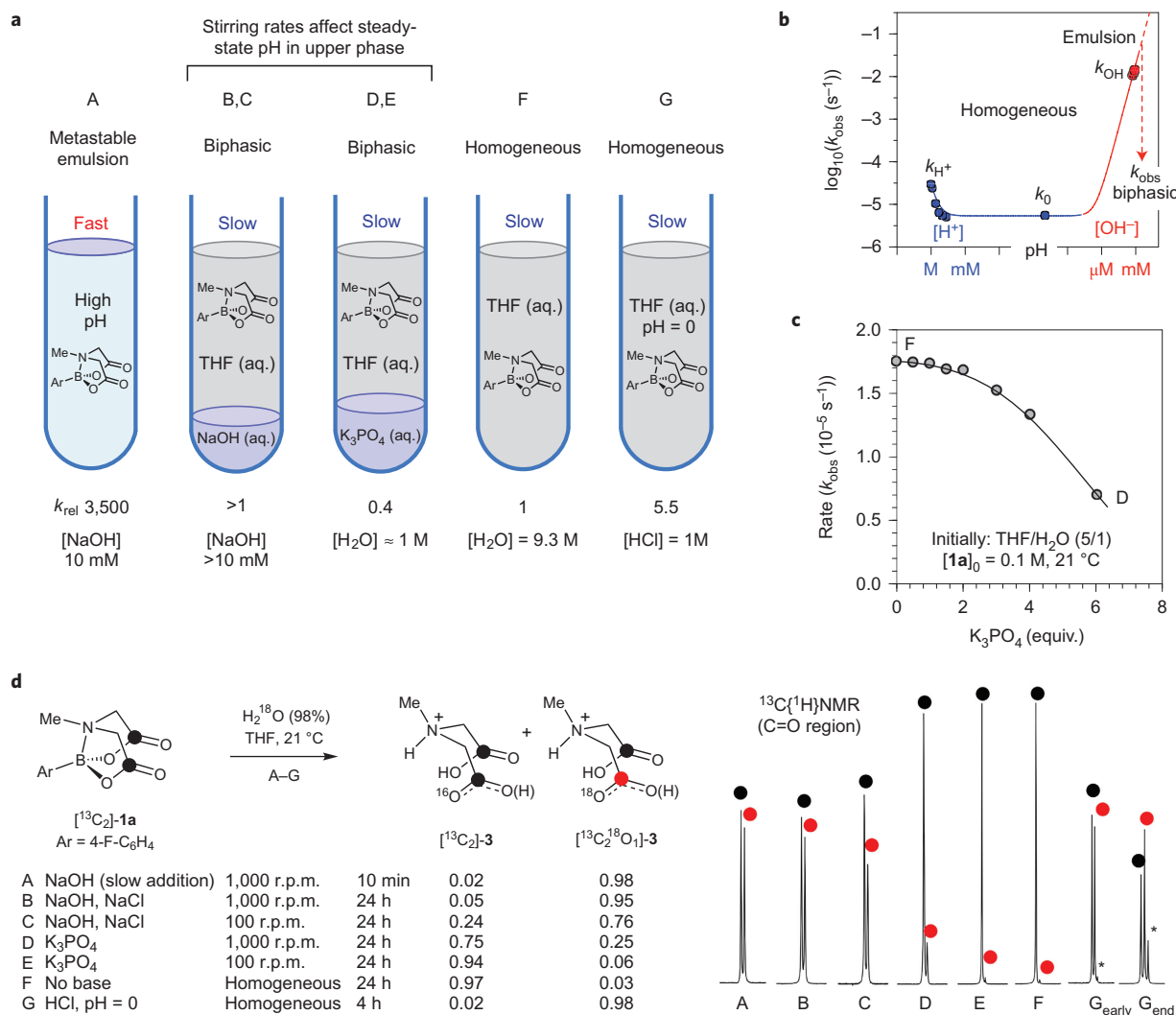


**Figure 2 | Distinction of limiting pathways for basic (fast, A), neutral (slow, F) and acidic (G) hydrolysis of **1a**.** **a**, Schematic representation of conditions A to G. **b**, pH rate profile, arbitrary pH scale (autoprotolysis constant of 0.5 mol fraction aqueous THF estimated as  $\text{pK}_{\text{app}} = 20$ )<sup>29</sup>. Hydrolysis of water-soluble Me-B(MIDA) in aqueous buffer (pH 1–11) confirms  $k_{\text{obs}} = k_{\text{H}^+}[\text{H}^+] + k_0 + k_{\text{OH}^-}[\text{OH}^-]$ . **c**, Impact of  $\text{K}_3\text{PO}_4$  on the hydrolysis rate under heterogeneous conditions. The line through the data is an aid to the eye. **d**,  $^{13}\text{C}\{^1\text{H}\}\text{NMR}$  subspectra (178.70–178.85 ppm;  $\Delta\delta^{18}\text{O}/^{16}\text{O} = 30$  ppb) of MIDA ligand (**3**) from the hydrolysis of  $[\text{C}_2]\text{-1a}$  in  $\text{THF}/^{18}\text{OH}_2$  under conditions A to G. Supplementary Figs 4 and 5 confirm a slow  $^{18}\text{O}$  exchange in **1a** but not in **3** under acidic conditions ( $G_{\text{early}}$ , 25% conversion;  $G_{\text{end}}$ , >98% conversion), and no exchange in **1a** and a very slow  $^{18}\text{O}$  exchange in **3** ( $\leq 1.4\%$ , 48 hours) under neutral conditions.  $^{13}\text{C}_2,^{18}\text{O}_2\text{-1a}$  that arises from slow exchange in **1a**.

The kinetics of neutral hydrolysis ( $k_0$ ) were measured across a wide range of water concentrations (0.5–20 M). Clean pseudo-first-order decays in **1a** ( $k_{\text{obs}}$  ( $\text{s}^{-1}$ )) were observed in all cases; however, despite the hydrolysis being slow, the determination of an overall rate law was not straightforward (Fig. 3b).

Analysis of  $k_{\text{obs}}$  as a function of water concentration gave a profile in which there is a rate plateau, suggestive of a change in the rate-limiting step, as might occur if pre-dissociation of the B–N bond in **1a** to give a reactive ‘open-**1a**’ intermediate was involved. However, this was not consistent with the entropy of activation ( $\Delta S^\ddagger = -16 \text{ cal K}^{-1} \text{ mol}^{-1}$ , 9.0 M  $\text{H}_2\text{O}$ ) and tests for open-**1a**, using diastereoselectively deuterated [ $^2\text{H}_{1,6}\text{-1a}$ ] were negative (Fig. 3c). Indeed, [ $^2\text{H}_{1,6}\text{-1a}$ ] required heating to 100 °C before significant rates of interconversion with *iso*-[ $^2\text{H}_{1,6}\text{-1a}$ ] were detected ( $\Delta G^\ddagger = 31 \text{ kcal mol}^{-1}$ ). Moreover, near-identical kinetic isotope effects (KIEs, *vide infra*, were obtained for the hydrolysis of **1a** at 0.5 M and at 9.1 M  $\text{H}_2\text{O}$ , above and below the rate plateau, suggestive of mechanistic continuity. Aqueous THF forms non-ideal mixtures<sup>13</sup> and, by the inclusion of a higher-order term for the water activity ( $a_w$ )<sup>14</sup>, the kinetic dichotomy is resolved (Fig. 3b). The resulting

correlation ( $k_0 = k'(a_w)^{2.8}$ ) suggests a rate-limiting attack of **1a** by water clusters ( $\text{H}_2\text{O}$ )<sub>n</sub> with average  $n = 2.8$ . The linear free-energy relationship for neutral hydrolysis ( $\log(k_X/k_{\text{H}}) = 0.8\sigma$ , 9.1 M  $\text{H}_2\text{O}$ ) indicates a moderate charge accumulation at the aromatic ring, as, for example, in a partially developed boronate anion.

**KIEs.** Further information on the sites of attack of **1a** (at C versus at B) during the rate-limiting events ( $k_{\text{OH}}$ ,  $k_0$  and  $k_{\text{H}^+}$ ) was deduced from KIEs. Heavy-atom KIEs were determined by double-labelling and analysing [ $^1\text{H}_4$ ]/[ $^2\text{H}_4$ ] ratios in [aryl- $^2\text{H}_n(\text{B},\text{C},\text{N})\text{-1a}$ ] mixtures ( $\Delta\delta_F = 0.56 \text{ ppm}$ ) as a function of fractional conversion. First-order competitive rates ( $k_{\text{rel}}$ ) were extracted by nonlinear regression and corrected for independently determined  $^2\text{H}$ -KIEs to yield  $^{10/11}k_{\text{B}}$ ,  $^{12/13}k_{\text{C}}$  and  $^{14/15}k_{\text{N}}$  under basic, neutral and acidic conditions (Fig. 4a–d).

For basic hydrolysis ( $k_{\text{OH}}$ ), a syringe-pump addition of aqueous NaOH, via a submerged narrow bore needle, into a vigorously stirred solution of **1a** (10 mM) ensured that reactions proceeded in a basic aqueous–organic emulsion prior to phase separation.

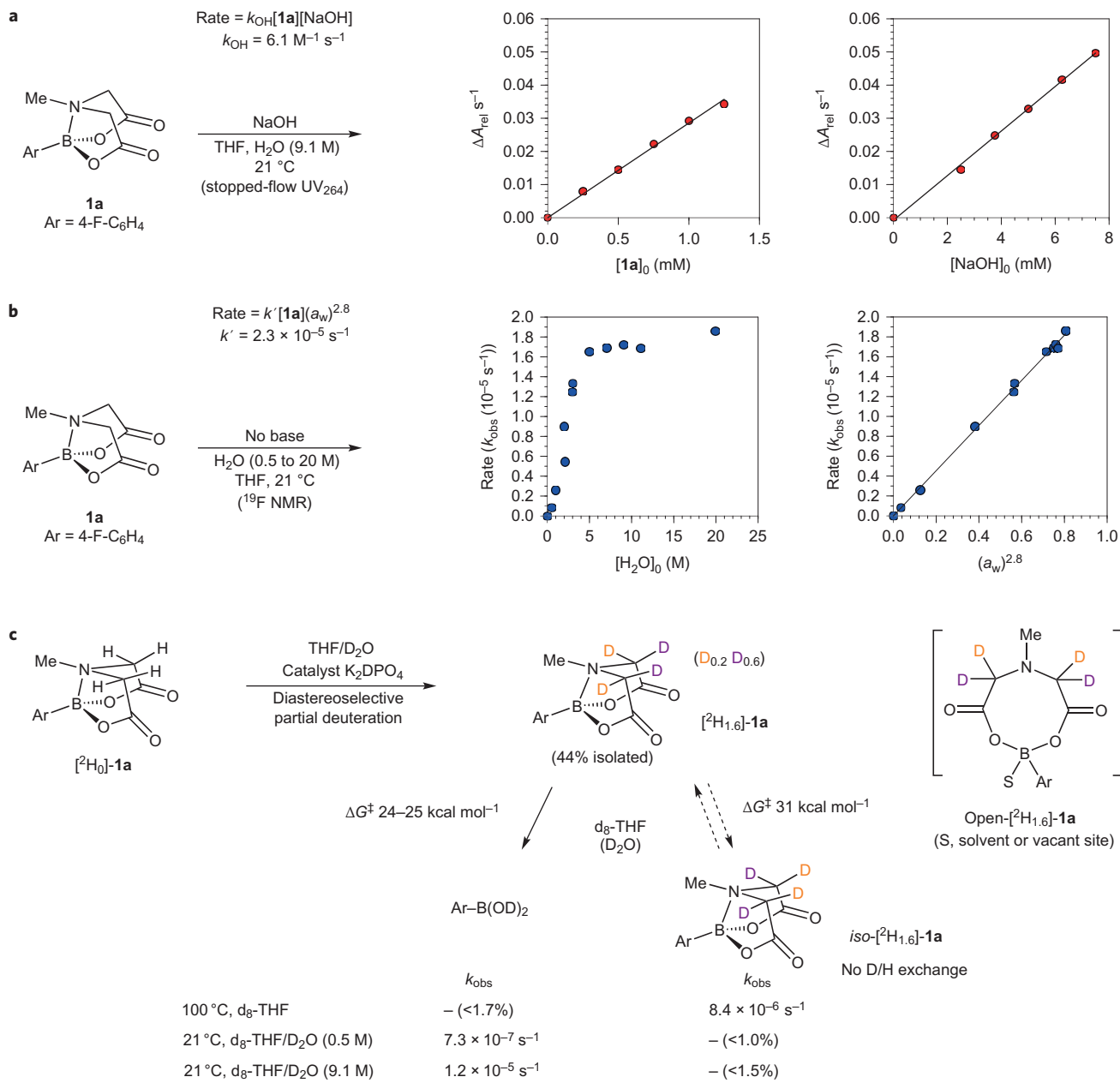


**Figure 3 | Kinetics of fast and slow hydrolysis of MIDA boronate **1a**.** **a**, Homogeneous basic conditions analysed by stopped-flow ultraviolet (UV) absorption spectrophotometry ( $\Delta A_{264} (\text{s}^{-1})$ ). Oxidation<sup>30</sup> of nascent **2a** to the phenol (4-F-C<sub>6</sub>H<sub>4</sub>OH) is accounted for in the analysis. **b**, Homogeneous neutral conditions, analysed by <sup>19</sup>F NMR. Hydrolysis rates correlate with water activity,  $k_0 = k'(a_w)^{2.8}$ ;  $k' = 2.3 \times 10^{-5} \text{ s}^{-1}$ , 21 °C. As hydrolysis proceeds, nascent zwitterion **3** either precipitates from solution ( $[\text{H}_2\text{O}] \leq 3 \text{ M}$ ), or induces minor phase separation. Control experiments confirmed these phenomena had negligible impact on the rates. **c**, Tests (negative) for open **1a** under conditions of homogeneous neutral hydrolysis.

The KIE (<sup>12/13</sup> $k_C = 1.049$  (Fig. 4b)) together with the rate law indicate that a carbonyl group in **1a** is attacked by hydroxide in the rate-determining step, without the direct involvement of either B or N. The outcome for acid-catalysed hydrolysis was analogous (<sup>12/13</sup> $k_C = 1.041$  (Fig. 4c)), indicative of rate-limiting ester hydrolysis ( $k_{\text{H}^+}$ ), albeit much less efficient ( $k_{\text{H}^+}/k_{\text{OH}} = 1 \times 10^{-5}$ ).

For neutral hydrolysis ( $k_0$ ), the KIEs (<sup>10/11</sup> $k_B = 1.032$  and <sup>14/15</sup> $k_N = 1.017$  (Fig. 4d)) are complementary to those for the acid/base mechanisms, with no KIE detected at carbon. A proton inventory<sup>15</sup> (Fig. 4e) for neutral hydrolysis ( $k_0$ ) in H<sub>2</sub>O/D<sub>2</sub>O/THF identified simultaneous primary ( $k_{\text{H/D}} = 1.59$ ) and secondary ( $k_{\text{H/D}} = 0.84$ ) KIEs; the effect of deuteration on the water activity in the neutral reaction ( $k_0$ ) is expected to be negligible<sup>16</sup>. The three normal primary KIEs ( $k_{\text{H}}$ ,  $k_B$  and  $k_N$ ) indicate that an O–H

bond in the attacking water cluster, (H<sub>2</sub>O)<sub>n</sub>, is cleaved in the rate-determining event, and that the B–N bond, not the carbonyl unit, in **1a** is involved in this process. The inverse secondary  $k_{\text{H/D}}$  arises from changes in solvation and hydrogen bonding of the residual (non-transferred) water proton(s)<sup>17</sup>.

## Discussion

**Pathways for hydrolysis.** The data reported above allow a large number of mechanistic possibilities to be ruled out. The unassisted cleavage of B–N to generate open-**1a** (Fig. 3c) is 6–12 kcal mol<sup>-1</sup> greater in energy than the experimentally determined hydrolysis rates ( $k_{\text{OH}}$ ,  $k_0$  and  $k_{\text{H}^+}$ ) and thus eliminates S<sub>N</sub>1-like pathways. Processes consistent with the rate-limiting events are an attack of **1** at the carbonyl carbon by OH<sup>-</sup> ( $k_{\text{OH}}$ ) or H<sup>+</sup>/H<sub>2</sub>O ( $k_{\text{H}^+}$ ), and at

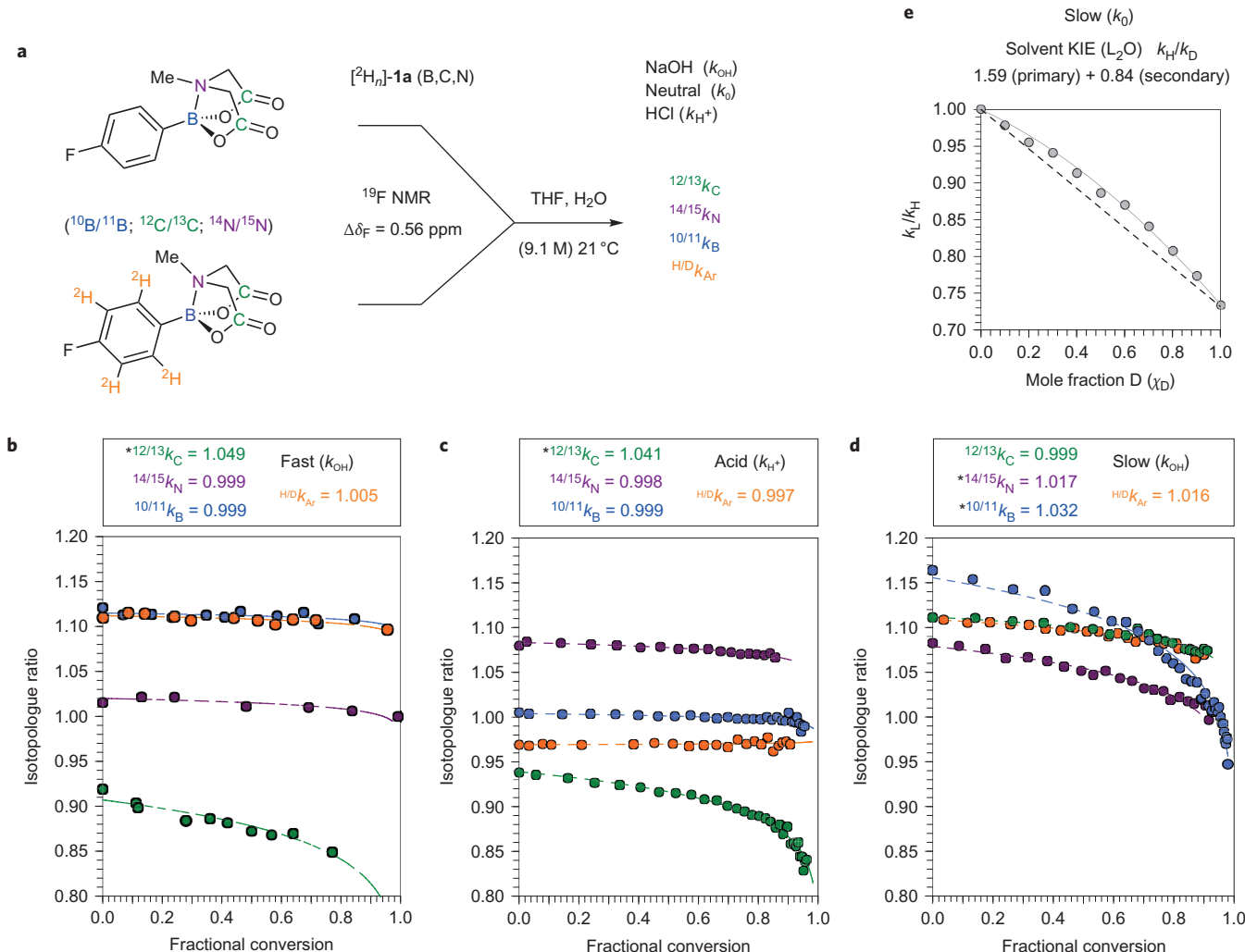


**Figure 4 | KIEs for Ar-B(MIDA) (1a) hydrolysis.** **a**, Outline of the methodology that allows KIE values to be extracted by a standard pseudo first-order competition model; the heavy-atom KIEs shown are those after correction for aryl deuteration<sup>31,32</sup>, net  $\sigma_D = -6.3(\pm 0.15) \times 10^{-3}$  and the competing processes ( $k_{\text{H}^+} + k_0$ ). **b**, Fast hydrolysis: substoichiometric aqueous NaOH added to vigorously stirred solutions of **1a** (10 mM) to attain a suitable span of fractional conversions. Hydrolysis after phase separation is inhibited by the addition of anhydrous MgSO<sub>4</sub>. **c**, Acidic hydrolysis (1 M HCl) analysed *in situ*. **d**, Neutral hydrolysis analysed *in situ*. Identical KIEs ( $\Delta \leq \pm 0.002$ ) were obtained with 0.5 M H<sub>2</sub>O. **e**, Proton inventory conducted with **1a** in THF/L<sub>2</sub>O (9.1 M, L = H, D). The net solvent KIE ( $\chi_D = 1$ ) increases from 1.4 to 2.0 as [D<sub>2</sub>O] is decreased from 9.1 to 0.5 M. \*Significant KIE.

the B–N unit by water ( $k_0$ ). The slow ( $k_{\text{H}^+}$ ) or undetected ( $k_{\text{OH}}$  and  $k_0$ ) rates of <sup>16/18</sup>O exchange in **1a** are inconclusive, as the oxygen atoms in the tetrahedral intermediates remain inequivalent, irrespective of proton-exchange rates<sup>18</sup>. Nonetheless, in none of the hydrolyses were intermediates detected by NMR (<sup>1</sup>H, <sup>19</sup>F and <sup>11</sup>B) or ultraviolet absorption (isosbestic points), which suggests that after the rate-limiting addition of ( $\text{H}^+/\text{H}_2\text{O}$ ), OH<sup>-</sup> or ( $\text{H}_2\text{O}$ )<sub>n</sub>, hydrolytic evolution to the boronic acid (**2a**) and MIDA ligand (**3**) is rapid. Substantial additional insight to the fast-release ( $k_{\text{OH}}$ ) and slow-release ( $k_0$ ) pathways relevant to coupling conditions<sup>2,3</sup> was gained by computations using Gaussian 09<sup>19</sup> at the M06-2X/6-31G\*/PCM (THF) level of theory<sup>20–22</sup>. In Figs 5a and 6a we provide a summary of the key stages of the two pathways identified. Below both pathways we also outline some of the other processes considered. Full details of these pathways are provided in Supplementary Figs 33–64.

In the fast-release ( $k_{\text{OH}}$ ) pathway, the minimum-energy pathway begins with the rate-limiting, irreversible attack by hydroxide at one of the two ester carbonyls in **1a** (C attack, TS-5,  $\Delta G^\ddagger = 2.2 \text{ kcal mol}^{-1}$  (Fig. 5a)). A fast ( $\Delta G^\ddagger \leq 5 \text{ kcal mol}^{-1}$ ), highly exothermic, irreversible collapse of the now tetrahedral

carbonyl carbon (TS-7) generates the ring-opened intermediate **8** ( $\Delta G = -29.9 \text{ kcal mol}^{-1}$ ).

As a result of the presence of a pendent carboxylate and of the increased lability of the B–N bond, **8** is substantially more prone to hydrolysis than neutral **1a**. Stage 2 hydrolysis proceeds via the attack of **8** at the boron by water (TS-9,  $\Delta G^\ddagger = 10.6 \text{ kcal mol}^{-1}$ ), which leads to **10**, and thus to the final products **2a** and **3** via B–O bond cleavage and ionization/salt formation. A NaOH-mediated rate-limiting C=O attack is consistent with experiment (computed <sup>12/13</sup>K<sub>C</sub> KIE, 1.03), the low sensitivity to aryl substituents ( $\rho = 0.5$ ) and the absence of experimentally observable <sup>14/15</sup>K<sub>N</sub> or <sup>10/11</sup>K<sub>B</sub> KIEs.

In the slow-release ( $k_0$ ) pathway, the minimum-energy pathway begins with the rate-limiting insertion of water into a stretching, but not cleaved, B–N bond (frontside-B-S<sub>N</sub>2 attack, TS-12 (Fig. 6a),  $+25.7 \text{ kcal mol}^{-1}$ ). At higher water concentrations, B–N cleavage by ( $\text{H}_2\text{O}$ )<sub>n</sub>,  $n = 1, 2$  or 3, has similar free-energy barriers, and the KIEs for these were computed with a range of levels of theory<sup>23</sup>. The best quantitative agreement was found in a late transition state using M06L/6-311++G\*\*. As the B–O bond is formed, to a great degree, with significant proton transfer to the nitrogen, there is negative charge accumulation at B ( $\rho$  0.4 to 1.0).

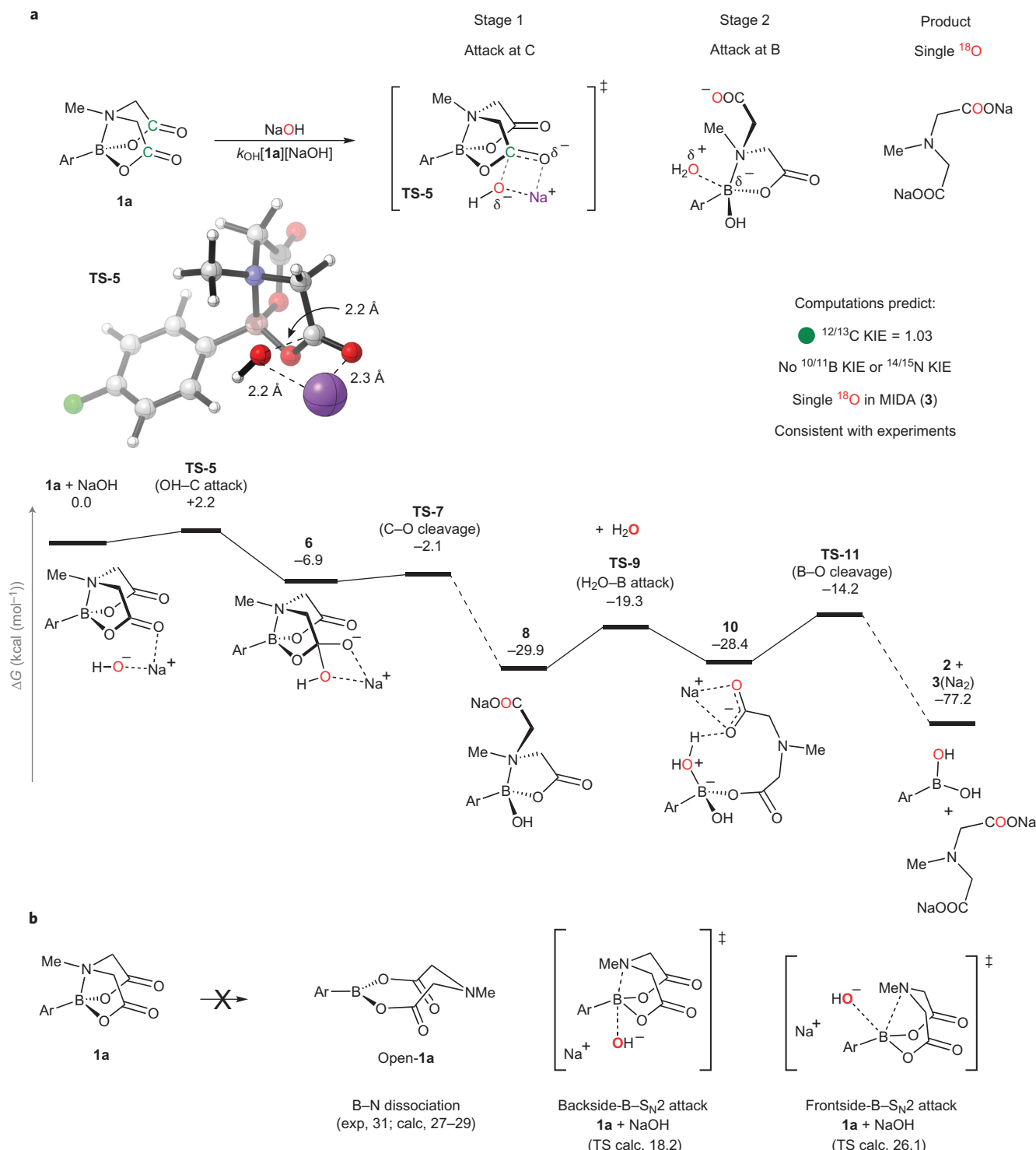


**Figure 5 | Fast-release hydrolysis ( $k_{\text{OH}}$ ).** **a**, Summary of key computational data for the hydrolysis of  $1\mathbf{a}$  via C–O bond cleavage (TS-5). The computed minimum-energy pathway and experimental data are fully self-consistent. Nonetheless, these computed results do not resort to exhaustive, time-dependent sampling, and should thus be taken only as a model of the processes that take place in the solution. **b**, Other key processes that were considered, but eliminated on the basis of energy or KIEs.

Stage 2 hydrolysis again involves a ring-opened intermediate (15), which, via intramolecular deprotonation of boron-coordinated water (TS-18), rapidly leads to complete hydrolysis. Rate-limiting B–N cleavage by H<sub>2</sub>O is consistent with experiment (computed KIEs  $^{14/15}\text{N}$  1.01,  $^{10/11}\text{B}$  1.03,  $^{1/2}\text{H}$  0.9 and 1.4), the sensitivity to aryl substituents ( $\rho$  = 0.8) and the absence of experimentally observable  $^{12/13}\text{C}$  KIE.

We also extensively probed alternative mechanisms for the fast and slow hydrolysis, at both the first and second stages. For stage one of the fast hydrolysis (Fig. 5b), B–N bond cleavage by backside-B-S<sub>N</sub>2 or frontside-B-S<sub>N</sub>2 attack of hydroxide is disfavoured over TS-5 by  $\geq 16$  kcal mol $^{-1}$ . The barrier for attack of 8 by hydroxide in stage two, at carbon or at boron (the latter being slightly favoured,  $\Delta\Delta G^{\ddagger} = 2.2$  kcal mol $^{-1}$ ), is also prohibitively high. The

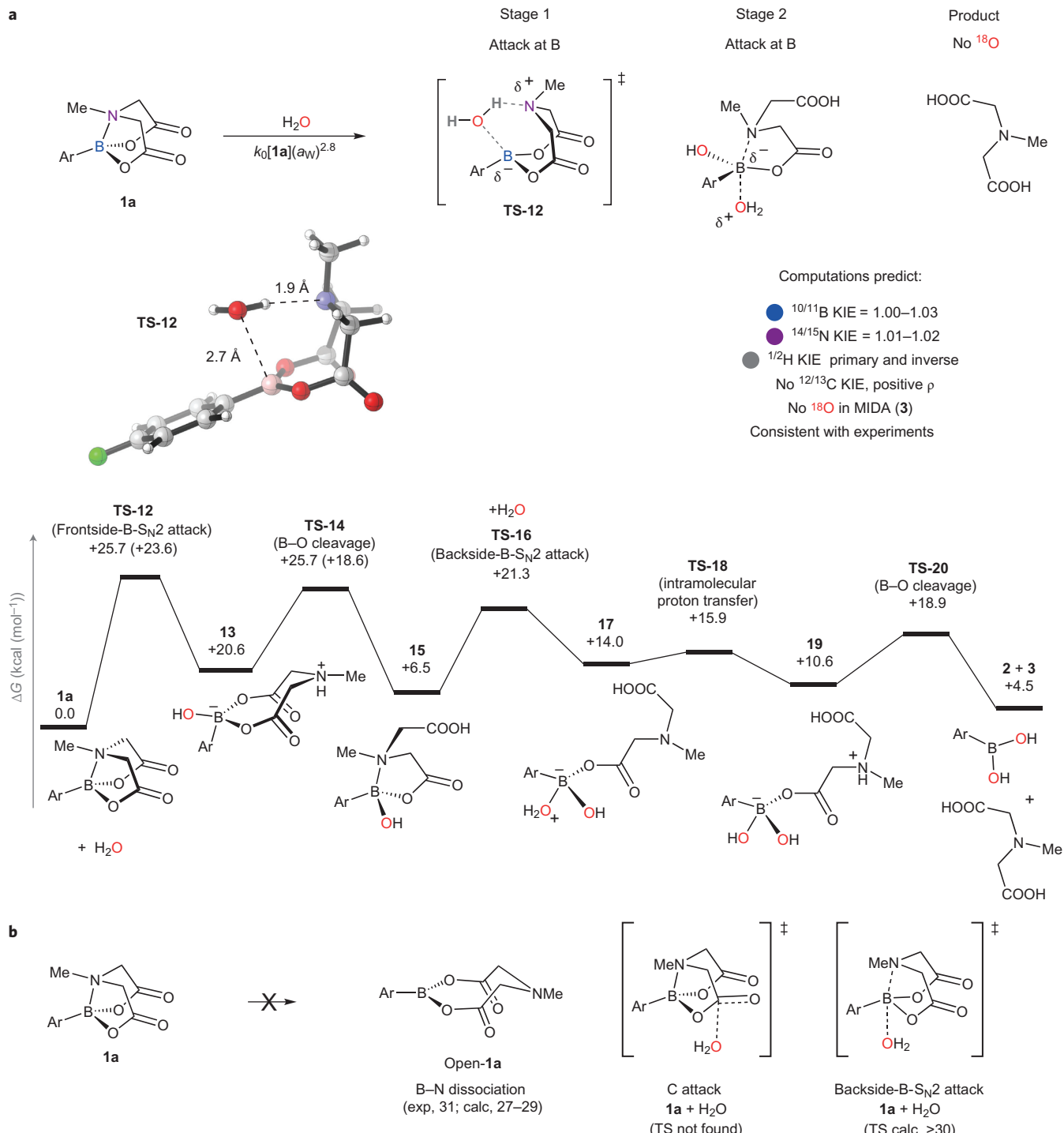


**Figure 6 | Slow-release hydrolysis ( $k_0$ ). a**, Summary of key computational data for the hydrolysis of **1a** via B-N bond cleavage (TS-12). The computed minimum-energy pathway and experimental data are fully self-consistent. Nonetheless, these computed results do not resort to exhaustive, time-dependent sampling, and should thus be taken only as a model of the processes that take place in the solution. **b**, Other key processes that were considered, but eliminated on the basis of energy or KIEs.

kinetics, KIEs and  $^{18}\text{O}$  incorporations indicate that a similar overall pathway (attack of a  $\text{C}=\text{OH}^+$  intermediate by  $\text{H}_2\text{O}$ , and then attack at B) operates under acid catalysis ( $k_{\text{H}^+}$ ). Slow hydrolysis ( $k_0$ ) proceeds without exogenous acid or base, and no transition state for  $\text{H}_2\text{O}$  attack at carbon (C attack (Fig. 6b)) could be located. Nonetheless, simple esters do slowly hydrolyse in pure water ( $\Delta G^\ddagger = 21-28 \text{ kcal mol}^{-1}$ )<sup>24</sup>, a process for which water chains<sup>24,25</sup> and water autoionization mechanisms ( $\Delta G^\ddagger = 23.8 \text{ kcal mol}^{-1}$ ) (ref. 26) have been proposed. Thus, irrespective of whether hydrolytic

cleavage ( $k_0$ ) of B-N in **1a** ( $\Delta G^\ddagger = 23.6 \text{ kcal mol}^{-1}$ ) involves transient water autoionization or concerted transfer (as in TS-12), appropriate dynamic fluctuations of water chains<sup>27</sup> will be required to facilitate it.

An alternative mechanism for stage one slow hydrolysis involves backside-B-S<sub>N</sub>2 attack (Fig. 6b), which leads to a weakly bound complex, from which water deprotonation by carboxylate cleaves the B-O bond. This is computed to have a higher energy barrier than frontside-B-S<sub>N</sub>2 attack (TS-12) and to result in a large

primary KIE ( $^{1/2}k_{\text{H}} \approx 3.8$ ), inconsistent with experiment (Fig. 4e and Supplementary Table 26). Overall, the differing rates and sites of the first-stage attack ( $\text{OH}^-$  at C in **TS-5** versus  $\text{H}_2\text{O}$  at B–N in **TS-12**) can be rationalized by: (1) hydroxide being much more nucleophilic than water ( $k_{\text{OH}}[\text{OH}] \gg k_0[\text{H}_2\text{O}]_n$ ), (2) the anionic charge from the attacking hydroxide being delivered to an electrophilic site (C=O) and (3) that B–N in **1** can simultaneously function as a Brønsted base and Lewis acid to provide a ‘receptor’ for activating water. After the stage-one rate-limiting processes ( $k_{\text{OH}}$ ,  $k_0$  and  $k_{\text{H}^-}$ ), all the pathways converge at stage two, albeit with different net charges, with flexible ring-opened intermediates (for example, **8** and **15**) that provide intramolecular assistance to the hydrolysis at boron.

**MIDA boronate hydrolysis under the conditions of application.** We have identified two general mechanisms (ester versus B–N cleavage) for the hydrolysis of **1a** operating under basic, neutral and acidic conditions. Of these,  $k_{\text{OH}}$  is by far the most efficient, becoming the major pathway when  $[\text{NaOH}] \geq 3 \mu\text{M}$ . At the concentrations used for synthesis, the conditions for fast and slow release (Fig. 1) result in separation into aqueous and organic phases. Maintaining high rates of fast release ( $k_{\text{OH}}$ ) is assisted by the generation of a transient emulsion, usually attained by vigorous agitation during a slow dispersive addition of aqueous NaOH. In the fully phase-separated medium, boronate (**1a**) undergoes a slow hydrolysis in the bulk organic–aqueous upper phase, the rate being mildly dependent on stirring and the mass-transfer rates between phases, and on  $a_w$  in the bulk organic phase. This detailed mechanistic understanding of the rate-limiting events for both hydrolysis pathways, and the physicochemical factors that govern their partitioning, enable rationalization of many of the phenomenological observations previously recorded with the MIDA platform.

The more than three orders of magnitude difference in rate attainable for fast versus slow hydrolysis results from the distinct mechanisms that underlie these processes. The remarkable insensitivity of these rates to the structure of the appended organic fragment is consistent with a minimal charge build-up at the boron centre during the attack at the carbonyl in the fast-release process and the presence of a common intramolecular base for facilitating the insertion of water into the N–B bond in the slow-release process. The stability of MIDA boronates in anhydrous solvents in the presence of inorganic bases, essential for iterative coupling, is consistent with the requirement for substantial water in the organic phase to promote neutral hydrolysis. MIDA boronates that bear exceptionally lipophilic organic fragments induce an accelerated phase separation when treated with NaOH, which results in a more-rapid switching to neutral hydrolysis and thus significantly extended reaction times for their complete hydrolysis. The slow-release cross-coupling of boronic acids proceeds via MIDA boronate hydrolysis in the upper aqueous–organic phase, whereas the inorganic base remains in the lower aqueous phase. The rates of hydrolysis under these slow-release conditions are highly reliable because the activity of water in THF<sup>14</sup> and in dioxane<sup>28</sup> is approximately constant ( $a_w \approx 0.8–1.0$ ) above concentrations of 3.0 M. The stability of MIDA boronates to many acidic conditions is consistent with their substantially slower rates of hydrolysis observed at low versus high pH.

Practically, this advanced mechanistic understanding also stands to enable a more effective and widespread utilization of MIDA boronates in synthesis. For example, simply increasing the dielectric constant of aqueous phases during reaction workups should help avoid the undesired hydrolysis of MIDA boronates in organic phases and thereby enable more-effective iterative cross-couplings as well as building-block syntheses. Using hydroxide salts that are more organic soluble should help further generalize the rates of MIDA boronate deprotections via fast hydrolysis, even for highly

lipophilic MIDA boronate intermediates. The rates of the slow release of unstable boronic acids from their MIDA boronate counterparts<sup>3</sup> can now be tuned rationally by simply varying the conditions to increase or decrease the contribution of basic versus neutral hydrolysis mechanisms. Using buffered HPLC eluents should maximize the MIDA boronate stability during the analysis and purification. This same understanding forms the basis for the rational design of new MIDA boronate analogues in which both modes of hydrolysis are deliberately retarded or accelerated by modifications to the iminodiacetic acid backbone. Broadly, such ligands stand to enable advanced applications of organoboron compounds in synthesis, including expanding the range of reaction conditions compatible with complex building-block construction and iterative assembly, opening new opportunities for selective boron deprotections and even one-pot pre-programmed iterative synthesis, and facilitating a transition in automation platforms from batch to flow chemistry. Such efforts can also now be guided by quantitatively tracking the relative contributions of the mechanisms of hydrolysis ( $k_{\text{OH}}/k_0$ ) simply by determining the  $^{18}\text{O}$  incorporation in the cleaved ligands (**3**) when conducting reactions in labelled water. Collectively, these advances stand to assist powerfully in the development of a more general and automated approach for small-molecule synthesis.

## Methods

Full experimental procedures, computational details, experimental data and computational discussion are provided in the Supplementary Information.

**General.** Density functional theory (DFT) calculations of the full reaction profiles for MIDA boronate solvolysis in basic and neutral aqueous THF were conducted at the M06-2X/6-31G\* level of theory with solvation using a polarized continuum model (PCM) for THF. The level of theory that provided the best quantitative agreement between predicted and observed KIEs for  $k_0$  was M06L/6-311+G\*\* with solvation in both THF and water computed as a single point using the default PCM settings in Gaussian 09<sup>19</sup> combined with the same level of theory. The MIDA boronates were prepared from the correspondingly labelled boronic acids (**2a**,  $^2\text{H}_4\text{-2a}$ ,  $^{10}\text{B}\text{-2a}$  and  $^{11}\text{B}\text{-2a}$ ) and N-methyliminodiacetic acids (**3**,  $^{15}\text{N}\text{-3}$  and  $^{13}\text{C}_2\text{-3}$ ) using standard procedures<sup>2</sup>, and purified via silica-gel column chromatography (Et<sub>2</sub>O/McCN 4:1) and then recrystallization (McCN-Et<sub>2</sub>O).

**Kinetics of MIDA boronate solvolysis in basic organic emulsion (fast release).** A stopped-flow system (TgK Scientific) was employed to deliver solutions of the isolated reactants (**1a**, 0.5–2.5 mM, and NaOH, 2.5–7.5 mM) in aqueous THF ( $[\text{H}_2\text{O}] = 9.1 \text{ M}$ ) in a 1:1 volume ratio via thermostatted reagent lines into a fused-silica ultraviolet-visible cuvette (pathlength 10 mm) with an integral pre-mixer (dead time <8 ms). Spectra were collected at 10 ms intervals on an Ocean Optics USB4000 detector and the data processed (Kinetic Studio, TgK Scientific) to afford the rate of change in absorbance (A) at 264 nm. To determine heavy-atom KIEs, samples of [aryl- $^2\text{H}_n$ ]**1a**, as an approximately 1:1 mixture of  $n = 0$  and  $n = 4$ , with isotopically labelled MIDA boronate moieties ( $^{10}\text{B}/^{11}\text{B}/^{13}\text{C}_2/^{15}\text{N}$ ), in one or other sample, were dissolved in 50 ml THF to give a total concentration of 10 mM. 4,4'-bis-(CF<sub>3</sub>)-biphenyl was added as an internal standard. Aliquots (5 ml) were then transferred to round-bottom flasks and vigorously stirred (>1,000 revolutions per minute (r.p.m.)) as 1 ml of an aqueous solution of NaOH was added via a syringe pump through a narrow-bore needle for five minutes. A series of NaOH concentrations (1–30 mM) was delivered to the sequence of aliquots to attain a suitable range of fractional conversions under metastable locally emulsified conditions. Immediately after the addition of the requisite volume of NaOH solution, the reactions were chilled in ice and sufficient anhydrous MgSO<sub>4</sub> added to inhibit further hydrolysis (both  $k_{\text{OH}}$  and  $k_0$ ). The solutions were concentrated (40 °C, 150 mbar) to approximately 0.5 ml and the isotope ratio and conversion analysed by  $^{19}\text{F}$  NMR.

**Kinetics of solvolysis of MIDA boronate **1a** in the absence of exogenous base (slow release).** Reactions were conducted in 5 mm NMR tubes kept at a constant temperature ( $\pm 0.5$  °C) in a thermostatted environment. A 0.6x ml aliquot of a stock solution of MIDA boronate **1a** in THF containing 4-CF<sub>3</sub>-bromobenzene as the internal standard, followed by  $x$  ml of aqueous THF, were added to the tube to establish final concentrations of 0.1 M **1a** and 9.1 M H<sub>2</sub>O. The sample was mixed vigorously, a sealed glass capillary that contained dimethylsulfoxide (DMSO)-d<sub>6</sub> added, the NMR tube sealed (J-Young valve) and then inserted into the NMR spectrometer (Bruker Advance, 376.3 MHz  $^{19}\text{F}$ ). After the spectrometer had been  $^2\text{H}$ -frequency locked to DMSO-d<sub>6</sub>, a series of  $^{19}\text{F}$  NMR spectra was recorded. The spectra were processed, as a block, and the integration of the  $^{19}\text{F}$  NMR signals

(inter-free-induction decay delays  $>5T_1$ ) for the internal standard, **1a** and **2a** was used to calculate concentrations. The pseudo-first order rate constant ( $k_{\text{obs}}$ ) was obtained from plots of  $\ln([1\mathbf{a}]_0/[1\mathbf{a}]_t) = k_{\text{obs}}t$ ; correlations were generally excellent ( $r^2 \geq 0.99$ ). Reactions were conducted across a wide range of other initial water concentrations (0.5–20.0 M), and with mixtures of  $\text{H}_2\text{O}/\text{D}_2\text{O}$ ,  $[\text{L}_2\text{O}] = 9.1$  M. The same procedure was employed to determine heavy-atom KIEs, except that [ $\text{aryl}-^2\text{H}_n\text{-}1\mathbf{a}$ ], as an approximately 1:1 mixture of  $n = 0$  and  $n = 4$ , with isotopically labelled MIDA boronate moieties ( $^{10}\text{B}/^{11}\text{B}/^{13}\text{C}_2/\text{N}$ ), in one or other sample, was employed.

Received 16 February 2016; accepted 13 June 2016;  
published online 25 July 2016

## References

- Li, J., Grillo, A. S. & Burke, M. D. From synthesis to function via iterative assembly of *N*-methyliminodiacetic acid boronate building blocks. *Acc. Chem. Res.* **48**, 2297–2307 (2015).
- Gillis, E. P. & Burke, M. D. A simple and modular strategy for small molecule synthesis: iterative Suzuki–Miyaura coupling of B-protected haloboronic acid building blocks. *J. Am. Chem. Soc.* **129**, 6716–6717 (2007).
- Knapp, D. M., Gillis, E. P. & Burke, M. D. A general solution for unstable boronic acids: slow-release cross-coupling from air-stable MIDA boronates. *J. Am. Chem. Soc.* **131**, 6961–6963 (2009).
- Lennox, A. J. J. & Lloyd-Jones, G. C. Organotrifluoroborate hydrolysis: boronic acid release mechanism and an acid–base paradox in cross-coupling. *J. Am. Chem. Soc.* **134**, 7431–7441 (2012).
- Woerly, E. M., Roy, J. & Burke, M. D. Synthesis of most polyene natural product motifs using just 12 building blocks and one coupling reaction. *Nature Chem.* **6**, 484–491 (2014).
- Li, J. *et al.* Synthesis of many different types of organic small molecules using one automated process. *Science* **347**, 1221–1226 (2015).
- Dick, G. R., Woerly, E. M. & Burke, M. D. A general solution for the 2-pyridyl problem. *Angew. Chem. Int. Ed.* **51**, 2667–2672 (2012).
- Fyfe, J. W. B., Seath, C. P. & Watson, A. J. B. Chemoselective boronic ester synthesis by controlled speciation. *Angew. Chem. Int. Ed.* **53**, 12077–12080 (2014).
- Li, J. & Burke, M. D. Pinene-derived iminodiacetic acid (PIDA): a powerful ligand for stereoselective synthesis and iterative cross-coupling of  $C(sp^3)$  boronate building blocks. *J. Am. Chem. Soc.* **133**, 13774–13777 (2011).
- Grob, J. E. *et al.* One-pot C–N/C–C cross-coupling of methyliminodiacetic acid boronyl arenes enabled by protective enolization. *Org. Lett.* **14**, 5578–5581 (2012).
- Gillis, E. P. & Burke, M. D. Multistep synthesis of complex boronic acids from simple MIDA boronates. *J. Am. Chem. Soc.* **130**, 14084–14085 (2008).
- Bender, M. L. & Thomas, R. J. The concurrent alkaline hydrolysis and isotopic oxygen exchange of a series of *p*-substituted methyl benzoates. *J. Am. Chem. Soc.* **83**, 4189–4193 (1961).
- Blandamer, M. J., Engberts, J. B. F. N., Gleeson, P. T. & Reis, J. C. R. Activity of water in aqueous systems; a frequently neglected property. *Chem. Soc. Rev.* **34**, 440–458 (2005).
- Treiner, C., Bocquet, J.-F. & Chemla, M. Seconds coefficients du viriel des mélanges eau-tetrahydrofurane (THF) influence sur les coefficients d'activité de l'eau et du THF à 25 °C. *J. Chim. Phys. Chim. Biol.* **70**, 72–79 (1973).
- Krishtalki, L. I. On the theory of the 'proton inventory' method. *Mendeleev Commun.* **3**, 66–67 (1993).
- Glew, D. N. & Watts, H. Aqueous non-electrolyte solutions. Part XII. Enthalpies of mixing of water and deuterium oxide with tetrahydrofuran. *Can. J. Chem.* **51**, 1933–1940 (1973).
- Schowen, R. L. The use of solvent isotope effects in the pursuit of enzyme mechanisms. *J. Label. Compd. Radiopharm.* **50**, 1052–1062 (2007).
- Bender, M. L., Matsui, H., Thomas, R. J. & Tobey, S. W. The concurrent alkaline hydrolysis and isotopic oxygen exchange of several alkyl benzoates and lactones. *J. Am. Chem. Soc.* **83**, 4193–4196 (1961).
- Frisch, M. J. *et al.* Gaussian 09 (Gaussian, Inc. Wallingford, Connecticut, 1973).
- Zhao, Y. & Truhlar, D. G. The M06 suite of density functionals for main group thermochemistry, thermochemical kinetics, noncovalent interactions, excited states, and transition elements: two new functionals and systematic testing of four M06-class functionals and 12 other functionals. *Theor. Chem. Acc.* **120**, 215–241 (2008).
- Hariharan, P. C. & Pople, J. A. The influence of polarization functions on molecular orbital hydrogenation energies. *Theor. Chim. Acta* **28**, 213–222 (1973).
- Miertus, S., Scrocco, E. & Tomasi, J. Electrostatic interaction of a solute with a continuum. A direct utilization of *ab initio* molecular potentials for the revision of solvent effects. *Chem. Phys.* **55**, 117–129 (1981).
- Beno, B. R., Houk, K. & Singleton, D. A. Synchronous or asynchronous? An 'experimental' transition state from a direct comparison of experimental and theoretical kinetic isotope effects for a Diels–Alder reaction. *J. Am. Chem. Soc.* **118**, 9984–9985 (1996).
- Guthrie, J. P. Hydration of carbonyl compounds, an analysis in terms of multidimensional Marcus theory. *J. Am. Chem. Soc.* **122**, 5529–5538 (2000).
- Guthrie, J. P. & Pitchko, V. Hydration of carbonyl compounds, an analysis in terms of no barrier theory: prediction of rates from equilibrium constants and distortion energies. *J. Am. Chem. Soc.* **122**, 5520–5528 (2000).
- Gunaydin, H. & Houk, K. N. Molecular dynamics prediction of the mechanism of ester hydrolysis in water. *J. Am. Chem. Soc.* **130**, 15232–15233 (2008).
- Geissler, P. L., Dellago, C., Chandler, D., Hutter, J. & Parrinello, M. Autoionization in liquid water. *Science* **291**, 2121–2124 (2001).
- Besbes, R., Ouerfelli, N. & Latrous, H. Density, dynamic viscosity, and derived properties of binary mixtures of 1,4 dioxane with water at  $T = 298.15$  K. *J. Mol. Liq.* **145**, 1–4 (2009).
- Woolley, E. M., Hurkot, D. G. & Hepler, L. G. Ionization constants for water in aqueous organic mixtures. *J. Phys. Chem.* **74**, 3908–3913 (1970).
- Butters, M. *et al.* Aryl trifluoroborates in Suzuki–Miyaura coupling: the roles of endogenous aryl boronic acid and fluoride. *Angew. Chem. Int. Ed.* **49**, 5156–5160 (2010).
- Perrin, C. L. & Dong, Y. Secondary deuterium isotope effects on the acidity of carboxylic acids and phenols. *J. Am. Chem. Soc.* **129**, 4490–4497 (2007).
- Pehk, T., Kiirend, E., Lippmaa, E., Ragnarsson, U. & Grehn, L. Determination of isotope effects on acid–base equilibria by  $^{13}\text{C}$  NMR spectroscopy. *J. Chem. Soc. Perkin Trans. 2* 445–450 (1997).

## Acknowledgements

G.C.L.-J. is a European Research Council (ERC) Advanced Investigator. The research leading to these results has received funding from the ERC under the European Union's Seventh Framework Programme (FP7/2007–2013)/ERC grant agreement No. 340163, and the US National Institutes of Health. G.C.L.-J. and J.A.G. thank CONACYT and The University of Edinburgh for generous support. M.D.B. acknowledges financial support from the US National Institutes of Health (GM118185). P.H.-Y.C. is the Bert and Emelyn Christensen Professor of Oregon State University and acknowledges financial support from the Stone family and the US National Science Foundation (NSF, CHE-1352663). K.N.H. is the Saul Winstein Chair in Organic Chemistry at the University of California Los Angeles and acknowledges financial support from the US NSF (CHE-1059084). O.M.O. acknowledges Tartar research support. O.M.O. and P.H.-Y.C. also acknowledge computing infrastructure in part provided by the NSF Phase-2 CCI, Center for Sustainable Materials Chemistry (NSF CHE-1102637).

## Author contributions

Experimental work was conducted by J.A.G. and G.F.M. Computational work was conducted by O.M.O., N.R., P.H.-Y.C. and A.G.L. G.C.L.-J., M.D.B., P.H.-Y.C., A.G.L. and K.N.H. wrote the manuscript.

## Additional information

Supplementary information is available in the online version of the paper. Reprints and permissions information is available online at [www.nature.com/reprints](http://www.nature.com/reprints). Correspondence and requests for materials should be addressed to P.H.Y.C., M.D.B. and G.C.L.-J.

## Competing financial interests

The University of Illinois has filed patent applications related to MIDA boronate chemistry, and these have been licensed to REVOLUTION Medicines, a company for which M.D.B. is a founder and consultant.